The Journal of Experimental Biology 203, 3445–3457 (2000)
Printed in Great Britain © The Company of Biologists Limited 2000
JEB2936

SOURCES AND MECHANISMS OF INORGANIC CARBON TRANSPORT FOR CORAL CALCIFICATION AND PHOTOSYNTHESIS

PAOLA FURLA[1], ISABELLE GALGANI[1], ISABELLE DURAND[1] AND DENIS ALLEMAND[1,2,*]

[1]*Observatoire Océanologique Européen, Centre Scientifique de Monaco, Avenue Saint-Martin, MC 98000 Monaco, Principality of Monaco* and [2]*UMR INRA-UNSA 1112, Université de Nice Sophia-Antipolis, BP 71, F-06108 Nice Cedex 02, France*

*Author for correspondence (e-mail: allemand@unice.fr)

Accepted 29 August; published on WWW 24 October 2000

Summary

The sources and mechanisms of inorganic carbon transport for scleractinian coral calcification and photosynthesis were studied using a double labelling technique with $H^{14}CO_3$ and ^{45}Ca. Clones of *Stylophora pistillata* that had developed into microcolonies were examined. Compartmental and pharmacological analyses of the distribution of ^{45}Ca and $H^{14}CO_3$ in the coelenteron, tissues and skeleton were performed in dark or light conditions or in the presence of various seawater HCO_3^- concentrations.

For calcification, irrespective of the lighting conditions, the major source of dissolved inorganic carbon (DIC) is metabolic CO_2 (70–75 % of total $CaCO_3$ deposition), while only 25–30 % originates from the external medium (seawater carbon pool). These results are in agreement with the observation that metabolic CO_2 production in the light is at least six times greater than is required for calcification. This source is dependent on carbonic anhydrase activity because it is sensitive to ethoxyzolamide. Seawater DIC is transferred from the external medium to the coral skeleton by two different pathways: from sea water to the coelenteron, the passive paracellular pathway is largely sufficient, while a DIDS-sensitive transcellular pathway appears to mediate the flux across calicoblastic cells. Irrespective of the source, an anion exchanger performs the secretion of DIC at the site of calcification. Furthermore, a fourfold light-enhanced calcification of *Stylophora pistillata* microcolonies was measured. This stimulation was only effective after a lag of 10 min. These results are discussed in the context of light-enhanced calcification.

Characterisation of the DIC supply for symbiotic dinoflagellate photosynthesis demonstrated the presence of a DIC pool within the tissues. The size of this pool was dependent on the lighting conditions, since it increased 39-fold after 3 h of illumination. Passive DIC equilibration through oral tissues between sea water and the coelenteric cavity is insufficient to supply this DIC pool, suggesting that there is an active transepithelial absorption of inorganic carbon sensitive to DIDS, ethoxyzolamide and iodide. These results confirm the presence of CO_2-concentrating mechanisms in coral cells. The tissue pool is not, however, used as a source for calcification since no significant lag phase in the incorporation of external seawater DIC was measured.

Key words: scleractinian, coral, *Stylophora pistillata*, biomineralization, anion transport, anion exchanger, carbonic anhydrase, compartment, carbon-concentrating mechanisms.

Introduction

Biomineralization is one of the most important biological processes in the living world. Nevertheless, calcification processes and, more specifically, mechanisms of ion transport largely remain a biological enigma. One of the major calcifying groups of organisms is the scleractinian corals. The rate of calcification of a coral reef is assumed to be approximately 10 kg $CaCO_3$ m^{-2} $year^{-1}$ (Chave et al., 1975), representing almost half the world's $CaCO_3$ precipitation (Smith, 1978), which has encouraged the use of corals as suitable models for biomineralization studies. Furthermore, the importance of coral reefs in the global cycling of carbonates (Smith, 1978) and their use as environmental archives (Barnes and Lough, 1996; Druffel, 1997) have stimulated research on the biology and physiology of scleractinian corals (for recent reviews, see Gates and Edmunds, 1999; Gattuso et al., 1999).

Coral skeleton formation results from the delivery of Ca^{2+} and inorganic carbon to the site of calcification. Tambutté et al. (1996) and Marshall (1996) have demonstrated that Ca^{2+} is delivered to the site of calcification by a transcellular transport process through the calicoblastic epithelium, pointing out the key role of biological control of biomineralization. Ca^{2+} uptake by this cell layer is mediated by L-type voltage-dependent Ca^{2+} channels (Zoccola et al., 1999) and Ca^{2+}-ATPases (Ip et al., 1991). This process is very rapid, Ca^{2+} transport from sea water

to the skeleton occurring within 1–2 min (Tambutté et al., 1996). However, there are few recent data describing the role of inorganic carbon in the biomineralization of corals.

After the pioneering work of Goreau (1961), who suggested that not all skeletal carbonate originates directly from dissolved inorganic carbon (DIC) in sea water, Pearse (1970) established that there are two different sources: (i) soluble carbonates from sea water and (ii) CO_2 produced by the metabolism of coral and zooxanthella tissue. Later, Erez (1978), using ^{45}Ca incorporation to measure *in situ* calcification rates in the coral *Stylophora pistillata*, found them to be 5–10 times higher than those determined using $H^{14}CO_3^-$, suggesting that metabolic CO_2 may represent up to 80 % of the carbon source in the presence of light. Moreover, Barnes and Crossland (1978) suggested that carbon transport results from transcellular transport and involves at least one intermediate compound. The scarcity of results reflects the methodological problems associated with the use of radioisotopes with corals (Barnes and Crossland, 1978). Most of these problems were overcome by using coral microcolonies in which the skeleton is entirely covered by tissues, thus avoiding direct radioisotope exchange between the sea water and the skeleton (Al-Moghrabi et al., 1993).

An understanding of DIC metabolism in relation to photosynthesis and calcification is of prime importance since DIC is a common substrate for both mechanisms. Furthermore, paleoenvironmental interpretations based on the stable isotope composition of coral skeleton have to take into account the 'vital effect' (Goreau, 1977), since both the chemical species used (HCO_3^- or CO_2) and the mode of transport (active *versus* passive) affect the isotopic fractionation. The purpose of this study was to determine the source(s) of carbon for photosynthesis and calcification, the mechanisms involved in its uptake, their kinetics and the characterization of the various carbon compartments. We have used a double labelling method (^{45}Ca and $H^{14}CO_3$) and a compartmental and a pharmacological approach derived from a protocol that we described previously (Tambutté et al., 1996).

Materials and methods

Biological material

Microcolonies were propagated in the laboratory from small fragments of *Stylophora pistillata* (Esper, 1797) collected at a depth of 5 m from the sea at the Marine Science Station, Gulf of Aqaba, Jordan. Corals were stored in an aquarium (300 l) supplied with sea water from the Mediterranean sea (exchange rate 2 % h^{-1}) heated to 25±0.1 °C and illuminated with a constant irradiance of 125–150 μmol photons m^{-2} s^{-1} using metal halide lamps (Philips HQI-TS, 400 W) on a 12 h:12 h light:dark photoperiod. Microcolony propagation has been described by Al-Moghrabi et al. (1993). Briefly, terminal portions of branches (6–10 mm long) were cut from the parent colonies and placed on a nylon net (1 mm×1 mm mesh) in the same conditions of light and temperature as the parent colonies. After approximately 1 month, coral fragments became entirely covered with new tissue.

Measurements of $^{45}Ca^{2+}$ and $H^{14}CO_3^-$ uptake and deposition

Labelling procedure

Isotope uptake was measured using a protocol described previously for ^{45}Ca alone (Tambutté et al., 1996) into three compartments: coelenteron, tissue and skeleton. Experiments were either performed in the dark (after at least 12 h in the dark) or in the light with an irradiance of 250 μmol photons m^{-2} s^{-1}. The composition of the solutions used for these studies is described below. Microcolonies were placed in plastic holders and incubated for 2–180 min in beakers with 10 ml of a labelled incubation medium (IM) containing ^{45}Ca and $H^{14}CO_3^-$. Magnetic stirring bars maintained water movement. A 100 μl sample of IM was removed before and after each incubation for the determination of total specific radioactivity (^{45}Ca plus inorganic ^{14}C), while 1 ml samples were removed for discrimination between the specific radioactivities of ^{45}Ca and inorganic ^{14}C (see below).

Measurement of the coelenteric compartment

At the end of the labelling period, each holder and its microcolony were immersed for 20 s in a beaker containing 600 ml of unlabelled efflux medium (EM) to prevent further isotope uptake and to reduce, by isotopic dilution, isotope adsorption. Labelled microcolonies were then placed in a beaker containing 30 ml of EM for 30 min. Upon completion of the efflux, a 100 μl sample of EM was collected for the determination of total radioactivity (^{45}Ca, organic ^{14}C and inorganic ^{14}C) and 2 ml was removed for discrimination between ^{45}Ca, organic ^{14}C and inorganic ^{14}C (see below). The radioactivity collected corresponds to the coelenteric compartment (for further details, see Tambutté et al., 1996).

Measurement of tissue and skeletal compartments

To separate tissues from skeleton, the microcolonies were heated at 90 °C for 20 min in 2 ml of 1 mol l^{-1} NaOH. Each skeleton was then rinsed with 1 ml of distilled water, which was collected and added to the dissolved tissues. A 100 μl sample of this solution, termed the 'tissue pool', was counted (total radioactivity: ^{45}Ca, organic ^{14}C and inorganic ^{14}C), a 500 μl sample was collected for protein measurements and 1 ml was used for discrimination between ^{45}Ca and inorganic ^{14}C.

Skeletons were processed according to the method described by Barnes and Crossland (1977). Briefly, clean skeletons were dissolved in 2 ml of 12 mol l^{-1} HCl. The resulting $^{14}CO_2$ was trapped on 200 μl of β-phenylethylamine absorbed onto two discs of Whatman GF/C filter paper in a scintillation vial connected to the test tube.

Sample processing

Measurement of the total radioactivity in the IM, EM and tissue pool samples was performed using a liquid scintillation counter (Tricarb, 1600 CA Packard) after the addition of 4 ml of the scintillation medium (Luma-gel; Packard). Since it is impossible to discriminate β emission from ^{45}Ca and from ^{14}C, the counting of a sample of double-labelled solution containing

both isotopes allows the total isotope content (^{45}Ca, inorganic ^{14}C and organic ^{14}C) to be measured.

To discriminate labelled inorganic carbon within IM, EM and the tissue pool from ^{45}Ca and from the organic ^{14}C fraction, we performed an acid titration of the samples collected. For this purpose, 200 µl of either 1 mol l^{-1} HCl (for IM and EM) or 12 mol l^{-1} HCl (for the tissue pool) was added to the reserved samples, resulting in the formation of $^{14}CO_2$. Active bubbling with air for 15 min induces the loss of all inorganic ^{14}C from the medium. The radioactivity of 100 µl of the solution was then determined using a liquid scintillation counter (Tricarb, 1600 CA Packard) after the addition of the scintillation medium (4 ml of Luma-gel, Packard) and neutralisation. This fraction represents ^{45}Ca and ^{14}C-labelled organic carbon. The ^{14}C-labelled inorganic carbon content was then calculated by subtracting the ^{45}Ca and ^{14}C-labelled organic carbon content from the total isotope content.

For skeletons, the HCl fraction (containing ^{45}Ca) was counted after the addition of 4 ml of Luma-gel (Packard) and neutralisation, while the filters (containing inorganic ^{14}C) were counted after the addition of 4 ml of scintillation medium (Ultima-Gold XR, Packard).

Consequently, the results presented below concerning ^{14}C uptake relate only to inorganic carbon, whereas the results concerning ^{45}Ca include both ^{45}Ca and ^{14}C-labelled organic compounds. This is particularly important in the tissue compartment in the light, where ^{45}Ca incorporation measures both the absorption of calcium and the fixation of carbon by photosynthesis. Since we cannot discriminate in the tissue between radioactive calcium and organic carbon, we have discarded results concerning ^{45}Ca measurement in the tissue pool in the light. However, preliminary experiments have shown that the incorporation of ^{14}C-labelled organic compounds into the skeleton in the light was insignificant compared with the incorporation of inorganic carbon and can, therefore, be discounted. Similarly, secretion of ^{14}C-labelled organic compounds into the coelenteron is low compared with the amount of ^{14}C-labelled DIC.

Measurement of photosynthetic and respiration rates

The rates of photosynthesis and respiration were measured as the net rate of O_2 production or consumption according to Bénazet-Tambutté et al. (1996b) using two micro-respirometers (Strathkelvin Instruments 928) each consisting of a double-walled cylindrical glass chamber (4 ml volume) and a Clark oxygen electrode (accurate to ±0.45 nmol O_2 ml^{-1}), with data output to a computer. Temperature was maintained at 25.0±0.5 °C using a recirculating water bath (Lauda RM20), and O_2 stratification was avoided using a magnetic stirring bar.

Media and chemicals

IM and EM constituted either normal filtered sea water (FSW) or sea water (SW) depleted of or enriched in HCO_3^-. In some experiments, inhibitors or competitors were added to the IM and EM. In each experiment, the IM and EM have the same composition, except that IM is a labelled medium containing 334–417 kBq of ^{45}Ca (supplied as $CaCl_2$, 1.38 MBq ml^{-1}; New England Nuclear) and 334–417 kBq of $H^{14}CO_3^-$ (supplied as $NaHCO_3$, 37 MBq ml^{-1}; New England Nuclear) while EM is an unlabelled medium. FSW was obtained by filtering Mediterranean sea water through a 0.45 µm Millipore membrane. Bicarbonate-free FSW ($0HCO_3$-FSW) was prepared according to Yellowlees et al. (1993). The pH of FSW was adjusted to 4.5 using 1 mol l^{-1} HCl to convert all DIC to CO_2. The CO_2 was removed by bubbling nitrogen through the FSW for approximately 1 h. The FSW was stirred throughout this procedure. The pH was then adjusted to 8.2 using 1 mmol l^{-1} Tris and CO_2-free NaOH prepared from a saturated NaOH solution to precipitate any sodium carbonate from solution. The buffer concentration did not interfere with the measurements (results not shown). FSW containing different concentrations of dissolved inorganic carbon was obtained by adding various concentrations of $NaHCO_3$ to $0HCO_3$-FSW before adjusting the pH and bubbling with air (Goiran et al., 1996). In all cases, the bicarbonate concentration was verified by calculation, according to the measured pH and total alkalinity (determined by the end-point titration acidometric technique using an alkalinity test; Merck).

4,4′-Diisothiocyanatostilbene-2,2′-disulfonic acid (DIDS), an anion carrier inhibitor (Cabantchik and Greger, 1992), was dissolved in dimethyl sulfoxide (DMSO) to obtain a stock solution of 100 mmol l^{-1}. The final concentration in FSW was 400 µmol l^{-1}. Ethoxyzolamide (EZ), a carbonic anhydrase inhibitor (Palmqvist et al., 1988), was dissolved in DMSO to a concentration of 60 mmol l^{-1} and buffered with 1 mol l^{-1} Tris to pH 8.2. The final concentration in FSW was 600 µmol l^{-1}. Although preliminary experiments demonstrated that concentrations of DMSO or ethanol up to 1 % (v/v) had no significant effect on dissolved inorganic carbon flux (results not shown), concentrations over 0.5 % were not used in the present study. Sodium iodide was used at a final concentration of 2 mmol l^{-1} as a competitor for HCO_3^- at the anion exchanger (Smith, 1988; Drechsler and Beer, 1991; Ilundain, 1992). All chemicals were obtained from Sigma or Merck.

Presentation of results

Results are expressed as nmol mg^{-1} protein in the NaOH-soluble pool and represent the mean ± S.E.M. for at least three replicates. Protein concentrations were measured in an autoanalyzer (Alliance Instruments) using the method of Lowry et al. (1951) and bovine serum albumin standards. One-way analysis of variance (ANOVA) with Bonferroni–Dunn *post-hoc* tests or Student's *t*-tests were used to evaluate differences between means (95 % confidence limits).

The half-time ($t_{1/2}$) of compartment loading and the affinity constant (K_m) were calculated graphically according to the curve-fitting program Mac-curve fit with exponential [$y=a(1-e^{-x/b})+c$] or Michaelis–Menten [$y=ax(x+b)+c$] equations. The flux into a given compartment was calculated according to Borle (1990) using the equations: unidirectional flux = k(compartment pool size) and $k=\log_e 2/t_{1/2}$.

Table 1. *Ca^{2+} and dissolved inorganic carbon pool sizes in the coelenteron and tissue compartments of* Stylophora pistillata *microcolonies incubated in the dark*

Compartment	Ca^{2+} pool size (nmol mg^{-1} protein)	Ca^{2+} pool $t_{1/2}$ (min)	DIC pool size (nmol mg^{-1} protein)	DIC pool $t_{1/2}$ (min)	*N*
Coelenteron	122.70±5.67	1	19.93±1.50	6.2	23
Tissue	39.35±2.01	53	5.83±0.75	72	19

N, the number of microcolonies analysed.
Values are means ± S.E.M.
$t_{1/2}$, half-time of compartment loading.

Results

Uptake and deposition of ^{45}Ca and ^{14}C in the dark

To determine the source of inorganic carbon for coral calcification and the kinetics of Ca^{2+} and DIC incorporation, we measured the rate of uptake of ^{45}Ca and ^{14}C into three compartments (coelenteron, tissues and skeleton). We first performed experiments in the dark to avoid any effects of photosynthesis. The rates of ^{45}Ca and ^{14}C uptake over 3 h in the dark by the coelenteric, tissue and skeletal compartments are depicted in Fig. 1. Ca^{2+} and DIC uptakes by both coelenteric and tissue compartments displayed saturable kinetics (Fig. 1A,B). In the coelenteron, equilibrium was reached for both isotopes after 15 min, but the $t_{1/2}$ for DIC was six times the $t_{1/2}$ for Ca^{2+}. In the tissue compartment, at least 3 h was necessary before equilibrium was attained for the two isotopes. The equilibrium values in the coelenteron and in the tissues for Ca^{2+} and DIC and the $t_{1/2}$ are summarised in Table 1. The equilibrium values represent the size of the exchangeable compartment for the two isotopes.

The time course of Ca^{2+} and HCO_3^- deposition in the skeletal compartment was linear for both isotopes for at least 3 h (Fig. 1C). No lag phase could be detected in the dark under our experimental conditions. The rate of Ca^{2+} incorporation in the dark (dark calcification rate) was 12.31±1.45 nmol h^{-1} mg^{-1} protein (*N*=23), whereas the rate of ^{14}C incorporation was 3.3 times lower, i.e. 3.77±0.77 nmol h^{-1} mg^{-1} protein (*N*=23).

Pharmacology of ^{45}Ca and ^{14}C-labelled DIC transport in the dark

To characterise the mechanisms of inorganic carbon absorption for coral calcification, we used inhibitors of anion transport (DIDS and iodide) and of carbonic anhydrase activity (EZ). These inhibitors did not affect the general metabolic rate, as indicated by the lack of any inhibitory action on the rate of respiration of *Stylophora pistillata* microcolonies in the dark (Table 2).

Fig. 2 shows the effect of DIDS, EZ and iodide on ^{45}Ca and ^{14}C incorporation into the tissue and skeletal compartments. The inhibitors did not affect the incorporation of isotopes in the coelenteric compartment (results not shown). ^{45}Ca and ^{14}C deposition in the skeleton was almost totally inhibited by 400 µmol l^{-1} DIDS, a blocker of anion transport (inhibition of 86±2 % and 89±2 % respectively; ANOVA, Bonferroni–Dunn *post-hoc* test, $P<0.0001$). Moreover, 2 mmol l^{-1} iodide, a competitor of HCO_3^- at anion exchangers, inhibited ^{45}Ca and ^{14}C skeletal incorporation equally (inhibition of 67±8 % and 65±7 % respectively; ANOVA, Bonferroni–Dunn *post-hoc* test, $P<0.0083$). Finally, EZ (600 µmol l^{-1}), a carbonic anhydrase inhibitor, potently blocked ^{45}Ca incorporation (by 56.04±6.98 %; ANOVA, Bonferroni–Dunn *post-hoc* test, $P<0.0083$), but had no effect on ^{14}C incorporation. In the inset of Fig. 2A, the ratio between ^{14}C and ^{45}Ca incorporation is presented as percentage of ^{14}C-labelled DIC *versus* ^{45}Ca incorporation. In control experiments, ^{14}C incorporation represented 25.56±4.11 % of calcification. No significant effect on this ratio was found in response to the addition of DIDS or iodide, while EZ induced an increase in the ratio (to 62.21±15.29 %; ANOVA, Bonferroni–Dunn *post-hoc* test $P<0.0083$).

Fig. 2B shows the effect of the inhibitors on isotope incorporation into the tissues. No significant effect of DIDS,

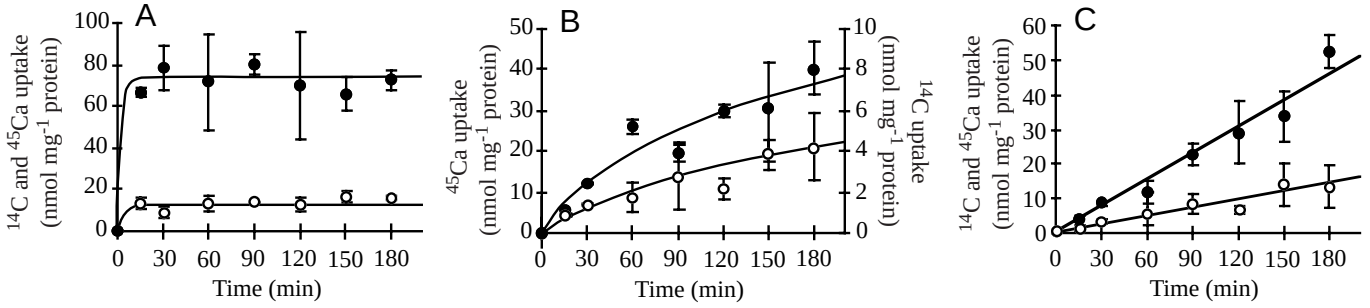

Fig. 1. Time course of ^{45}Ca (●) and ^{14}C (○) incorporation into the coelenteron (A), tissues (B) and skeleton (C) of *Stylophora pistillata* microcolonies measured in the dark. Values are expressed as means ± S.E.M. Four microcolonies were analysed for each point.

Table 2. *Rate of respiration in the dark of* Stylophora pistillata *in presence of DIDS, ethoxyzolamide and iodide*

Experimental conditions	Rate of respiration (nmol h^{-1} mg^{-1} protein)	*N*
Control	193.92±13.04	13
DIDS (400 µmol l^{-1})	240.25±23.69	4
Ethoxyzolamide (300 µmol l^{-1})	200.50±20.98	4
Iodide (2 mmol l^{-1})	171.00±29.41	4

None of the values is significantly different from the control (P>0.05).

N, the number of microcolonies analysed.

Values are means ± S.E.M.

iodide or EZ on the incorporation of ^{45}Ca and ^{14}C was observed.

Uptake and deposition of ^{45}Ca and ^{14}C in light-adapted microcolonies

A second set of experiments was performed in the light (250 µmol photons m^{-2} s^{-1}) to investigate the effects of photosynthesis on the source of inorganic carbon for calcification and on the mechanisms of carbon incorporation. Fig. 3 shows the kinetics of ^{45}Ca and ^{14}C incorporation over 1 h in the light in the coelenteric and skeletal compartments. Ca^{2+} and HCO_3^- uptake by the coelenteron displayed saturable kinetics (Fig. 3A). ^{45}Ca uptake equilibrated within approximately 2 min, while $H^{14}CO_3^-$ equilibration was achieved more slowly (8.6 min). In the tissue compartment, the uptake of ^{14}C-labelled DIC followed a sigmoidal time course, equilibrium being reached only after 3 h (Fig. 3B and inset). The equilibrium values in the coelenteron and in the tissues for Ca^{2+} and HCO_3^- and the kinetic constants are summarised in Table 3.

In the presence of light, the deposition of ^{45}Ca and of ^{14}C into the skeletal compartment was linear (Fig. 3C) and this for for at least 3 h (results not shown). No lag phase could be detected under our experimental conditions. The rate of Ca^{2+} incorporation in the light (light calcification rate) was 49.25±3.71 nmol h^{-1} mg^{-1} protein (N=36). The rate of

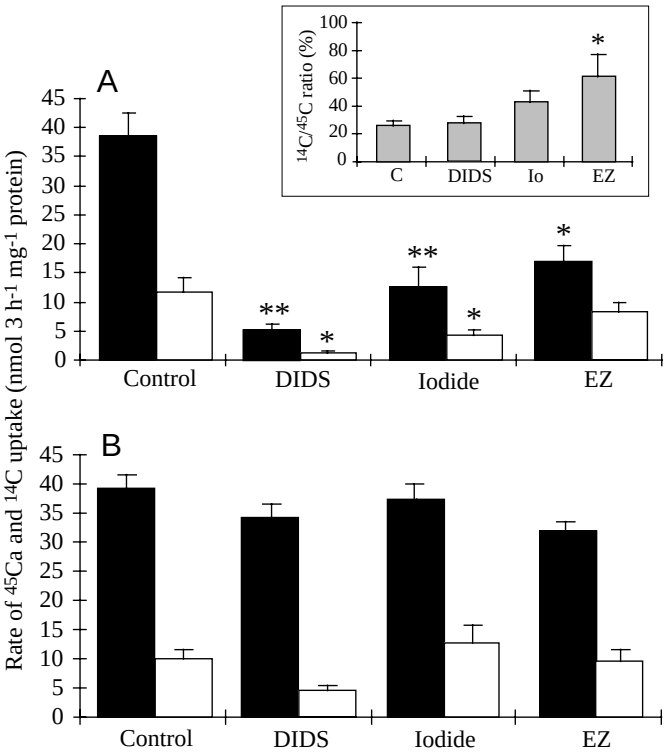

Fig. 2. Pharmacology of ^{45}Ca (filled columns) and ^{14}C (open columns) incorporation into the skeleton (A) and tissues (B) of *Stylophora pistillata* microcolonies in the dark. Effects of DIDS (400 µmol l^{-1}), an anion exchanger inhibitor, iodide (Io; 2 mmol l^{-1}), a competitor of HCO_3^- in anion transport, and ethoxyzolamide (EZ; 300 µmol l^{-1}), a carbonic anhydrase inhibitor. The inset shows the effects of these inhibitors on the ratio between ^{14}C incorporation and ^{45}Ca incorporation, reported as the percentage of ^{14}C-labelled dissolved inorganic carbon *versus* ^{45}Ca incorporation. Values are expressed as means + S.E.M. The number of microcolonies analysed was 23 for control experiments and 9–10 for experiments in the presence of an inhibitor. Results obtained in the presence of inhibitors were compared using one-way ANOVA and a Bonferroni–Dunn *post-hoc* test. Asterisks indicate values statistically different from the control: *P<0.0083, **P<0.0001. *C*, control.

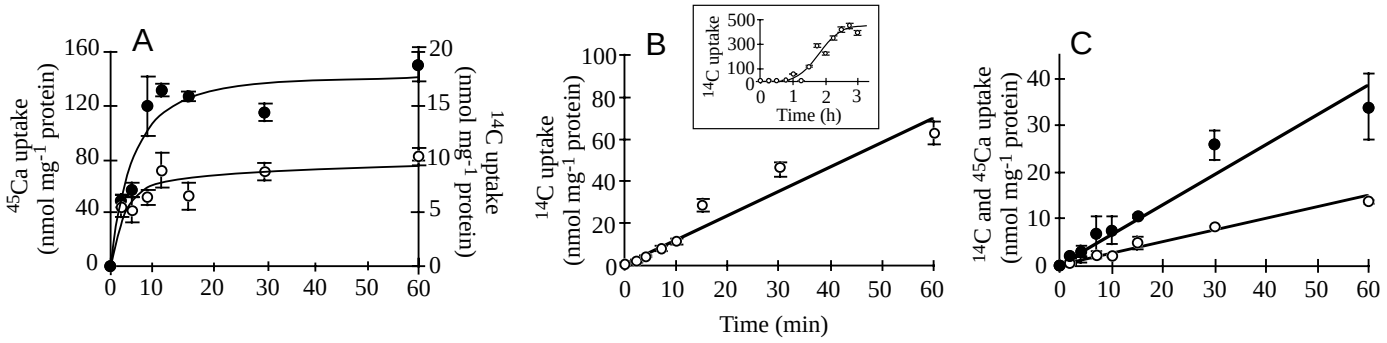

Fig. 3. Time course of ^{45}Ca (●) and ^{14}C (○) incorporation into the coelenteron (A), tissues (B) and skeleton (C) of *Stylophora pistillata* microcolonies measured in the presence of light (250 µmol photons m^{-2} s^{-1}). In the inset, the kinetics of incorporation of ^{14}C over 3 h is presented. Values are expressed as means ± S.E.M. Four microcolonies were analysed for each point.

Table 3. *Ca^{2+} and dissolved inorganic carbon pool sizes in the coelenteron and tissue compartments of* Stylophora pistillata *microcolonies incubated in the light*

Compartment	Ca^{2+} pool size (nmol mg^{-1} protein)	Ca^{2+} pool $t_{1/2}$ (min)	DIC pool size (nmol mg^{-1} protein)	DIC pool $t_{1/2}$ (min)	*N*
Coelenteron	93.86±2.42	2	12.87±1.28	8.6	29
Tissues	2069.25±81.48	13	229.46±42.73	106	32

N, the number of microcolonies analysed.
The light level was 250 µmol photons m^{-2} s^{-1}.
DIC, dissolved inorganic carbon.
The value of Ca^{2+} pool size of the tissues takes into account both ^{45}Ca and ^{14}C-labelled organic carbon.
Values are means ± S.E.M.
$t_{1/2}$, half-time of compartment loading.

^{14}C incorporation was 2.9 times slower, i.e. 17.14± 1.82 nmol h^{-1} mg^{-1} protein (*N*=36).

Effect of HCO_3^- concentration in the light

Fig. 4 shows ^{45}Ca and ^{14}C uptakes at external concentrations of HCO_3^- ranging from 0 to 3 mmol l^{-1}. While HCO_3^- uptake by the coelenteric compartment was linearly correlated (r^2=0.948, *P*=0.0002) with the external HCO_3^- concentration, coelenteric Ca^{2+} incorporation was not dependent (r^2=0.042, *P*=0.6978) on external [HCO_3^-] (Fig. 4A). In tissues, ^{14}C-labelled DIC uptake showed typical Michaelis–Menten saturable kinetics (K_m=0.2 mmol l^{-1}; Fig. 4B). The plateau (22.03±2.85 nmol h^{-1} mg^{-1} protein) was reached at an external HCO_3^- concentration of approximately 0.5 mmol l^{-1}. Fig. 4C shows that the rate of ^{45}Ca incorporation into coral skeleton became saturated at an external HCO_3^- concentration of approximately 1 mmol l^{-1}, while the rate of ^{14}C deposition into the skeleton was linear up to 3 mmol l^{-1} HCO_3^-.

Pharmacology of ^{45}Ca and ^{14}C-labelled DIC transport in the presence of light

Previous studies have shown that DIDS and EZ inhibit coral photosynthesis in the light (Al-Moghrabi et al., 1996), but no data are available on the effects of iodide. We therefore measured the rate of photosynthesis of microcolonies of *Stylophora pistillata* in the presence of 2 mmol l^{-1} sodium iodide. No difference in the rate of oxygen production in the absence or presence of this competitor was detected (179.71±23.08 and 172.47±8.51 nmol h^{-1} mg^{-1} protein, respectively, Student's *t*-test, *P*>0.05; result not shown).

Fig. 5 shows the effects of DIDS, EZ and iodide on ^{45}Ca and ^{14}C incorporation (in the light) into the skeletal (Fig. 5A) and tissue (Fig. 5B) compartments. As for experiments performed in the dark, no effect of these inhibitors on the uptake of isotopes was observed in the coelenteric compartment (results not shown), consistent with previous observations (Tambutté et al., 1996).

Fig. 5A shows that the deposition of ^{45}Ca and of ^{14}C into the skeleton was almost totally inhibited by DIDS (inhibition of 85±4 % and 97±1 %, respectively; ANOVA, Bonferroni–Dunn *post-hoc* test, *P*<0.0001). EZ also had an important inhibitory effect on the deposition of both isotopes (inhibition of 67±4 % and 62±6 %, respectively; ANOVA, Bonferroni–Dunn *post-hoc* test, *P*<0.0001). In contrast, only a small non-significant inhibition was observed in the presence of iodide. In the inset of Fig. 5A, the ratio between ^{14}C and ^{45}Ca incorporation is presented as the percentage of ^{14}C-labelled DIC *versus* ^{45}Ca incorporation. In control experiments, the incorporation of ^{14}C represented 36.6±3.2 % of the calcification. While no significant effect on the ratio was observed after the addition of iodide or EZ, exposure to DIDS induced a decrease in this

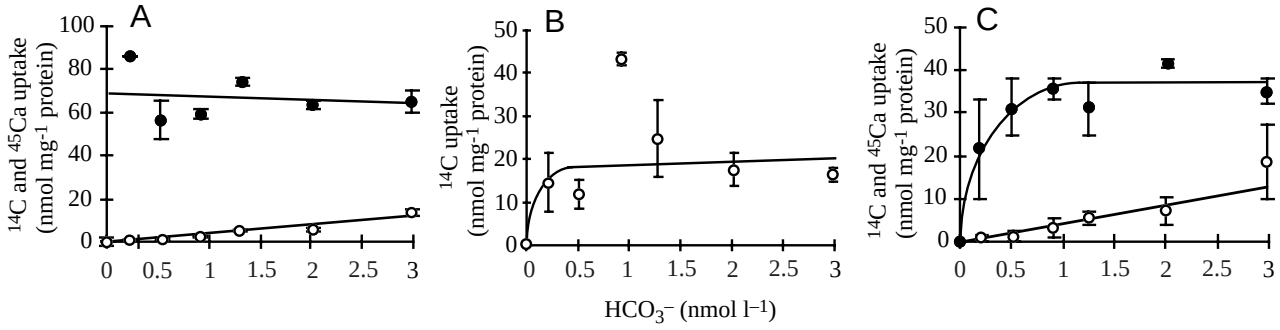

Fig. 4. External [HCO_3^-]-dependence of ^{45}Ca (●) and ^{14}C (○) incorporation into the coelenteron (A), tissues (B) and skeleton (C) of *Stylophora pistillata* microcolonies measured in the presence of light (250 µmol photons m^{-2} s^{-1}). Values are expressed as means ± S.E.M. Four microcolonies were analysed.

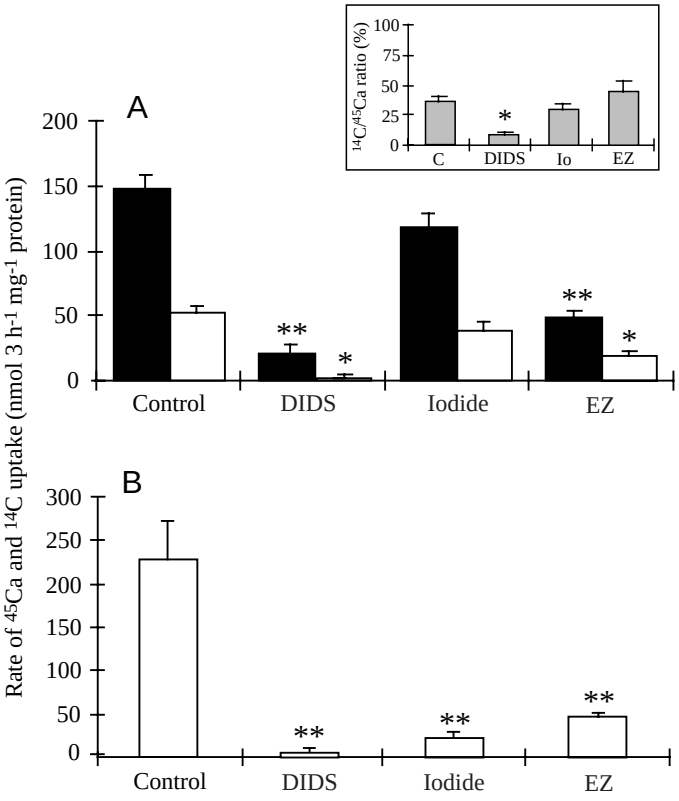

Fig. 5. Pharmacology of ^{45}Ca (filled columns) and ^{14}C (open columns) incorporation into the skeleton (A) and tissues (B) of *Stylophora pistillata* microcolonies in the presence of light (250 μmol photons m^{-2} s^{-1}). The effects of DIDS (400 μmol l^{-1}), an anion exchanger inhibitor, iodide (Io; 2 mmol l^{-1}), a competitor of HCO_3^- in anion exchangers, and ethoxyzolamide (EZ; 300 μmol l^{-1}), a carbonic anhydrase inhibitor, are shown. The inset shows the effects of these inhibitors on the ratio between ^{14}C incorporation and ^{45}Ca incorporation, reported as the percentage of ^{14}C-labelled dissolved inorganic carbon *versus* ^{45}Ca incorporation. Values are expressed as means + S.E.M. The number of microcolonies analysed was 36 for control experiments and 5–12 for experiments in the presence of inhibitors. Results obtained in the presence of inhibitors were compared using one-way ANOVA and a Bonferroni–Dunn *post-hoc* test. Asterisks indicate values statistically different from the control: **P*<0.0083, ***P*<0.0001. *C*, control.

ratio (to 9.2±2.3 %; ANOVA, Bonferroni–Dunn *post-hoc* test, *P*<0.0083). The results presented in Fig. 5B show that uptake of ^{14}C-labelled DIC by the tissue was almost totally inhibited by DIDS, iodide and EZ (by 100±1 %, 90±3 % and 80±2 %, respectively; ANOVA, Bonferroni–Dunn *post-hoc* test, *P*<0.0001).

Uptake and deposition of ^{45}Ca and ^{14}C in the presence of light after a dark period

Fig. 6 shows the kinetics of the incorporation of ^{45}Ca and ^{14}C into the three compartments over 1 h when microcolonies were placed in the light after having spent 12 h in the dark. Both Ca^{2+} and DIC uptake by the coelenteron displayed saturable kinetics (Fig. 6A,B), with equilibrium being reached within 4–10 min for both isotopes ($t_{1/2}$=1.8 min and 5.4 min, respectively, for Ca^{2+} and DIC). Upon illumination of the microcolonies, ^{14}C-labelled DIC uptake by the tissues was linear, whereas the incorporation of ^{45}Ca displayed a slight lag phase of approximately 4 min (Fig. 6C,D). Finally, Fig. 6E,F shows that the deposition of ^{45}Ca and ^{14}C into the skeleton of *Stylophora pistillata* follows biphasic kinetics: the rates were low during the first 10 min (0.55±0.06 nmol ^{45}Ca min^{-1} mg^{-1} protein and 0.058±0.015 nmol ^{14}C min^{-1} mg^{-1} protein) but subsequently increased (0.91±0.13 nmol ^{45}Ca min^{-1} mg^{-1} protein and 0.11±0.01 nmol ^{14}C min^{-1} mg^{-1} protein).

Discussion

Sources of inorganic carbon for calcification

In the present study, sources of inorganic carbon for calcification of *Stylophora pistillata* have been characterised and compared for microcolonies incubated in the dark or in the presence of light. Under both conditions, the rate of ^{45}Ca deposition into the coral skeleton was greater than the rate of ^{14}C incorporation (Figs 1C, 3C). The ratio ^{14}C/^{45}Ca expresses the incorporation of DIC originating from the external medium: a ratio of 1 (100 %) means that the same amounts of seawater DIC and Ca^{2+} are incorporated into the skeleton, while a lower value means that an unlabelled source of DIC is also used. In the present experiments, the ratio in the dark did not differ significantly from that in the light (25.56±4.11 % in the dark and 36.60±3.22 % in the light; Student's *t*-test, *P*>0.05). These results demonstrate that the inorganic carbon originating from the surrounding medium does not constitute the major source of DIC for coral calcification in either light or dark conditions. The labelled seawater DIC is likely to be diluted by unlabelled DIC originating from coral tissue. This unlabelled DIC could be either intracellular bicarbonate or metabolic CO_2, as suggested by Goreau (1961), Pearse (1970) and Erez (1978). The calcification rate remains constant for periods of at least 180 min (Figs 1, 3), ruling out the involvement of the tissue pool, the $t_{1/2}$ of which is less than 100 min (Tables 1, 3). Consequently, the unlabelled source of DIC must be the metabolic CO_2 produced by the symbiotic association.

A role for this metabolic CO_2 as source of carbon for calcification has already been demonstrated in non-symbiotic gorgonians (Allemand and Grillo, 1992; Lucas and Knapp, 1997) and in symbiotic corals (Crossland, 1980). Supporting this hypothesis, the calicoblastic cells, which are responsible for skeletogenesis, contain numerous mitochondria (Johnston, 1980; E. Tambutté, personal communication). Furthermore, measured respiration rates in *Stylophora pistillata* microcolonies (Table 2) show that metabolic CO_2 production (193.92±13.04 nmol h^{-1} mg^{-1} protein) is sufficient to support the metabolic inorganic carbon requirements for calcification in both dark and light conditions (8.54±1.64 nmol h^{-1} mg^{-1} protein and 32.11±4.13 nmol h^{-1} mg^{-1} protein, respectively, i.e. from 4.4 to at least 16.5 % of metabolic CO_2 production). Moreover, the respiration rate probably increases in the light

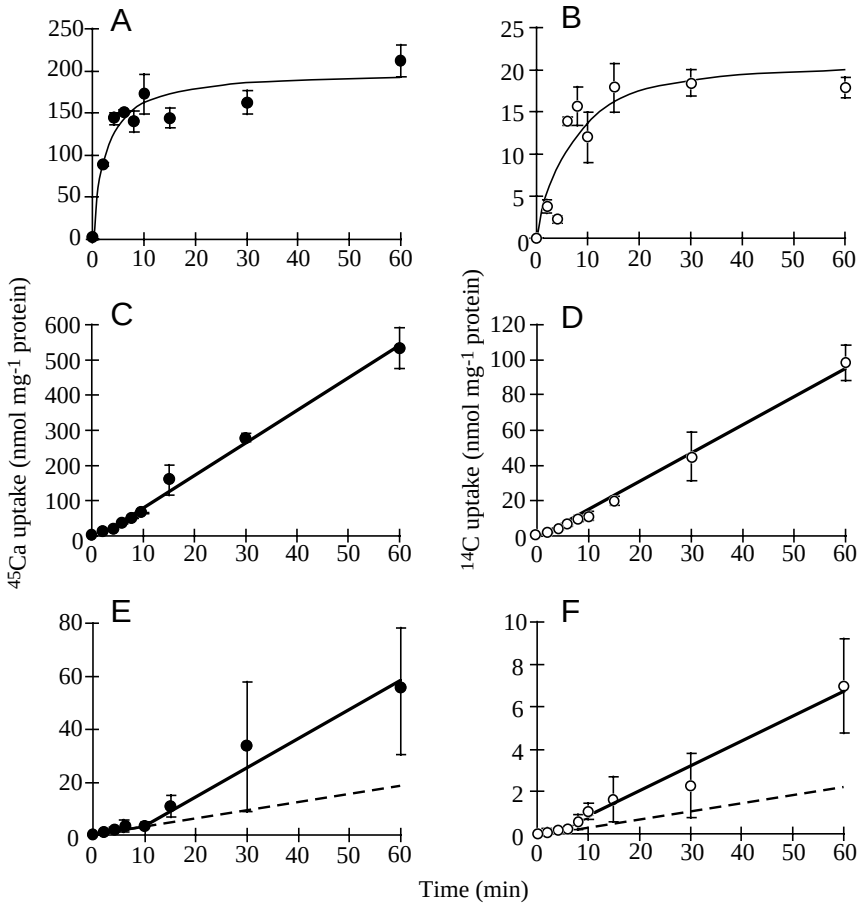

Fig. 6. Time course of ^{45}Ca (●) and ^{14}C (○) incorporation into the coelenteron (A,B), tissues (C,D) and skeleton (E,F) of *Stylophora pistillata* microcolonies measured in the presence of light (250 μmol photons m^{-2} s^{-1}) after a dark period of 12 h. Broken lines represent the extrapolated rate of Ca^{2+} and HCO_3^- incorporation into the skeletal compartment over the first 10 min of incubation. Values are expressed as means ± S.E.M. Four microcolonies were analysed for each point.

(Shick, 1990). While Goreau (1961) and Erez (1978) reported a $^{14}C/^{45}Ca$ ratio in the light similar to the ratio that we measured here (21 % and 22 %, respectively), their results differed in the dark. Erez (1978) determined that the major source of DIC in the dark was the external pool (mean dark $^{14}C/^{45}Ca$ ratio 93 %). However, his experiments were performed *in situ*, and there was marked variability in the results obtained, with the ratio in the dark varying between 28 and 100 %.

Our results demonstrate that the major source of DIC for calcification is the metabolic DIC pool irrespective of lighting conditions and, therefore, of photosynthesis. This result should be taken into account for paleoenvironmental studies using stable carbon isotopes since a predominant incorporation of metabolic CO_2 leads to the formation of a skeleton with a light isotopic composition, which does not reflect the situation in sea water.

Compartmental analysis of Ca^{2+} and dissolved inorganic carbon

Coelenteric Ca^{2+} and DIC analysis

Both in the dark and in the light, the equilibrium constant ($t_{1/2}$) for DIC in the coelenteron was higher than that for Ca^{2+} (Tables 1, 3). This is probably a consequence of the higher transepithelial permeability to Ca^{2+} compared with HCO_3^- (Bénazet-Tambutté et al., 1996a; Furla et al., 1998a). In the light, both equilibrium constants increased slightly compared with dark conditions (Tables 1, 3), suggesting that the permeability of the tentacles is probably reduced by light. These changes are probably due to a modification of the tissue thickness induced by light (Furla et al., 1998a). Absorption of both Ca^{2+} and DIC into the coelenteric cavity was insensitive to inhibitors of ion transport, suggesting that it occurs *via* passive diffusion. This was confirmed by the linear correlation between the external [HCO_3^-] and the coelenteric DIC pool (Fig. 4A). These results support the finding of Tambutté et al. (1996), who demonstrated that calcium uptake in the coelenteron is mediated by a paracellular pathway across the oral tissue.

From the size of the coelenteric DIC pool and the kinetic constant, it is possible to calculate the transepithelial DIC flux (see Materials and methods). In the dark, the passive transepithelial flux through oral tissues is 2.2 nmol min^{-1} mg^{-1} protein (i.e. 132 nmol h^{-1} mg^{-1} protein), while it is theoretically 1.03 nmol min^{-1} mg^{-1} protein (i.e. 62 nmol min^{-1} mg^{-1} protein) in the light. This passive transepithelial flux of DIC through oral tissues appears to be enough to support calcification even in the light (49 nmol min^{-1} mg^{-1} protein). However, this flux is far too small to support symbiont photosynthesis (180 nmol min^{-1} mg^{-1} protein), suggesting the need for active uptake of DIC by the oral tissue, in accordance with previous findings (Furla et al., 2000).

In the presence of light, the coelenteric DIC pool was

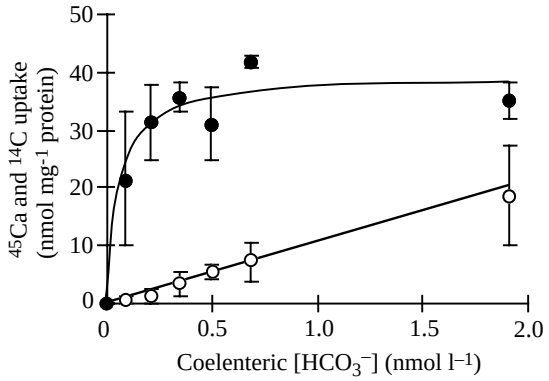

Fig. 7. Coelenteric [HCO_3^-]-dependence of ^{45}Ca (●) and ^{14}C (○) incorporation into the skeleton of *Stylophora pistillata* microcolonies measured in the presence of light (data from Fig. 4C). Values are expressed as means ± S.E.M. Four microcolonies were analysed.

decreased by approximately 44 % compared with dark conditions (Tables 1, 3). When equilibrium is reached between the Ca^{2+} concentration within the coelenteron and the sea water, it is possible to extrapolate the water volume of the coelenteron (Tambutté et al., 1996). From the data presented in Tables 1 and 3 concerning the coelenteric Ca^{2+} pool, and the specific radioactivity, water volumes of 10.76±0.78 µl mg^{-1} protein in the dark and 8.61±0.45 µl mg^{-1} protein in light were calculated. From these values, and knowing the size of the coelenteric HCO_3^- pool, it is possible to calculate the coelenteric concentration of HCO_3^-: 2.29±0.15 mmol l^{-1} in the dark and 1.29±0.05 mmol l^{-1} in the light. A similar light-dependent decrease in DIC concentration within body fluids has been described in symbiotic clams (Leggat et al., 1999) and may reflect the continuous uptake of DIC for both calcification and photosynthesis. Activation of photosynthesis in the presence of light probably induced, during the first few minutes of illumination, an instantaneous uptake of DIC from the coelenteric medium by endodermal cells, as previously demonstrated in the Mediterranean sea anemone *Anemonia viridis*. In this species, a comparable decrease in HCO_3^- concentration in the light (dark coelenteric DIC concentration 2.43±0.02 mmol l^{-1}, P. Furla and D. Allemand, unpublished data; light coelenteric DIC concentration 1.31±0.18 mmol l^{-1}; $P<0.05$, Furla et al., 1998b) and a simultaneous increase in the coelenteric pH to 9.0 (Furla et al., 1998b) have been measured. Since the DIC used for calcification necessarily originates from the coelenteron, the dependence of calcification on DIC (Fig. 4) can be redrawn using the calculated DIC concentration within the coelenteron (Fig. 7). Now, calcification appears to be saturated at low coelenteric HCO_3^- concentrations (approximately 200 µmol l^{-1}; K_m 60 µmol l^{-1}).

Consequently, the chemistry of inorganic carbon within the coelenteron is profoundly altered upon illumination. If we assume that the coelenteric pH varies at least from 7.5 (in the dark) to 8.5 (in the light), as measured by Kühl et al. (1995) and by Furla et al. (1998b), and taking into account changes in total DIC measured in the present study, it is possible to calculate the carbon species involved. In Table 4, we have summarised the main metabolic characteristics of *Stylophora pistillata*. These data show that CO_2 concentrations vary from 66 µmol l^{-1} in the dark to 3 µmol l^{-1} in the light, and that the saturation states of calcite and aragonite are increased by a factor 4.7 in the light.

Table 4. *Summary of the main characteristics of Ca^{2+} and dissolved inorganic carbon metabolism in* Stylophora pistillata *microcolonies in the dark or in light*

	Dark	Light
Rate of respiration (nmol h^{-1} mg^{-1} protein)	194	⩾194
Rate of photosynthesis (nmol h^{-1} mg^{-1} protein)	–	179
Rate of calcification (^{45}Ca) (nmol h^{-1} mg^{-1} protein)	12.31	49.25
Rate of calcification (^{14}C) (nmol h^{-1} mg^{-1} protein)	3.77	17.14
^{14}C/ ^{45}Ca in the skeleton (%)	26	37
Fraction of metabolic CO_2 used for calcification (%)	4.4	17
Water volume of the coelenteron (µl mg^{-1} protein)	10.8	8.6
Coelenteric pH*	7.5	8.5
Total coelenteric DIC (mmol l^{-1})	2.29	1.29
[HCO_3^-] in the coelenteron (mmol l^{-1})‡	2.17	1.02
[CO_2] in the coelenteron (µmol l^{-1})‡	66	3
[CO_3^{2-}] in the coelenteron (µmol l^{-1})‡	57	268
Calcite oversaturation in the coelenteron (%)‡	143	672
Aragonite oversaturation in the coelenteron (%)‡	79	372
[HCO_3^-] in tissues (mmol l^{-1})	3.7	147
$[DIC]_{intracellular}/[DIC]_{extracellular}$	1.56	61.30
Passive transepithelial oral DIC flux (nmol h^{-1} mg^{-1} protein)	132	62

*Values obtained by Kühl et al. (1995) and Furla et al. (1998b).

‡Calculated using the CO_2 program of M. Frankignoulle (University of Liège, Unité d'Océanographie Chimique) by assuming values of coelenteric pH similar to those measured by Kühl et al. (1995) and Furla et al. (1998b).

The light level was 250 µmol photons m^{-2} s^{-1}.

DIC, dissolved inorganic carbon.

Tissue Ca^{2+} and DIC analysis

The DIC equilibrium value in the tissues was reached in the light, as in the dark, after approximately 3 h (Fig. 1B, inset of Fig. 3B). Nevertheless, the DIC pool in the light was approximately 39 times larger than in the dark (Table 3). If we consider the cell water space measured by Bénazet-Tambutté et al. (1996a), i.e. 1.56 µl mg^{-1} protein, we can calculate the cellular concentration of DIC in the light and in the dark from the DIC tissue pool: 147 and 3.7 mmol l^{-1}, respectively.

Consequently, the ratio $[DIC]_{intracellular}/[DIC]_{extracellular}$ increases from 1.6±0.2 in the dark to 61.3±0.2 in the light. This increase is another argument supporting the proposition that a CO_2-concentrating mechanism is stimulated upon illumination, as previously suggested by Allemand et al. (1998). Furthermore, the ratio measured in the light (61.3) is within the range found in phototrophs possessing a CO_2-concentrating mechanism, which varies between 10 in some macrophytes to 16 000 in some cyanobacteria (Aizawa and Miyachi, 1986; Bowes and Salvucci, 1989).

Mechanisms of DIC transport for coral photosynthesis and calcification

In the presence of light, DIC accumulation is sensitive to DIDS, iodide and EZ, suggesting the involvement of an anion exchanger and carbonic anhydrase in the absorption of DIC for photosynthesis (Fig. 5B). While Furla et al. (2000) recommended that care should be taken regarding the specificity of DIDS in corals, the inhibitory effect of iodide confirms the involvement of anion exchangers. However, because the inhibitory effect of DIDS is greater than that of iodide, we cannot exclude the participation of an H^+-ATPase, as has been described previously in other symbiotic, but non-calcifying, cnidarians (Furla et al., 2000).

Pharmacological experiments performed in the dark allowed the determination of mechanisms by which DIC is transported for coral calcification independently of symbiont photosynthesis. The results presented in Fig. 2A show that the target of DIDS also plays an important role in the mechanisms of coral calcification, since the skeletal incorporation of Ca^{2+} and DIC was greatly inhibited by this blocker, as previously shown by Tambutté et al. (1996). However, previous studies have demonstrated that this inhibitor affects not only anion exchangers but also anion conductances and P-type H^+-ATPases (Furla et al., 2000). Consequently, it is possible that DIDS could also inhibit the Ca^{2+}-ATPase, another P-type ATPase (Forgac, 1989), responsible for the extrusion of Ca^{2+} from calicoblastic cells (Ip et al., 1991; Tambutté et al., 1996).

Nevertheless, the role of anion transport in $CaCO_3$ precipitation was confirmed by the inhibitory action of iodide. This competitor affected both Ca^{2+} incorporation into the skeleton and DIC incorporation, demonstrating that its target is involved in both external and metabolic DIC incorporation. Finally, EZ alters the ratio of seawater/metabolic DIC supply in the dark (inset of Fig. 2A) but is without effect on ^{14}C incorporation, suggesting that only the metabolic source of DIC is dependent on carbonic anhydrase activity. The inhibition of the metabolic source was partially compensated by the predominant absorption of external DIC (62 % of total $CaCO_3$ deposition instead of 25 %). In the light, similar results were obtained, suggesting that the mechanisms of calcification in the light are similar to those in the dark. However, while EZ had only a slight and insignificant stimulatory effect on the $^{14}C/^{45}Ca$ ratio, DIDS inhibited the supply of DIC from external sea water, and this was offset by an increase in the supply of metabolic CO_2 (inset of Fig. 5).

The present data suggest that, irrespective of its sources (external or metabolic), DIC uptake for symbiont photosynthesis and secretion by calicoblastic cells into the skeleton is dependent on an anion transport mechanism, indicating that HCO_3^- is the ionic species transported. Our results also demonstrate that the metabolic source of DIC is dependent on carbonic anhydrase, which catalyses the hydration of CO_2 to HCO_3^- in the calicoblastic cells, to prevent leakage of gaseous CO_2. After paracellular diffusion of DIC across the oral tissue, the uptake of external DIC into calicoblastic cells occurs by a mechanism that remains to be characterised.

Light-enhanced calcification

Numerous studies of coral calcification have demonstrated stimulation of $CaCO_3$ deposition in the light compared with the dark (for a review, see Gattuso et al., 1999). Similarly, in the present study, we have shown that the rate of calcification of *Stylophora pistillata* microcolonies in the light is 4.00±0.08 times greater than the rate of calcification in the dark (Figs 1C, 3C). Moreover, the application of blockers of photosynthesis led to an inhibition of this light-enhanced calcification. Incorporation of both isotopes was similarly stimulated. Interestingly, the enhancement of calcification was apparent only 10 min after the onset of illumination (Fig. 6). The kinetics of light-enhanced calcification has not been extensively studied. Barnes and Crossland (1978) measured a lag period of 35–45 min before inorganic carbon deposition was stimulated in the skeleton of *Acropora acuminata*. These authors suggested that this lag phase was an artefact arising from the dilution of ^{14}C by an unlabelled pool of DIC in the tissue. Our results are not consistent with such a hypothesis since we measured a lag phase for both ^{45}Ca and ^{14}C-labelled DIC deposition. Moreover, in the tissues, this lag phase was shorter (2–4 min) for both isotopes (Fig. 6C,D). Finally, the inorganic carbon present in the tissues was saturated after 60 min in the dark and after 150 min in the light, whereas the rate of calcification remained constant for at least 3 h. These results suggest the activation of mechanisms for DIC and Ca^{2+} absorption and/or deposition following illumination (Mueller, 1984).

Numerous hypotheses have been proposed to explain the stimulation of calcification by light (for a review, see Barnes and Chalker, 1990). The most relevant are light-enhanced calcification (Goreau, 1959; Allemand et al., 1998), dark-repressed calcification (Marshall, 1996) and trans-calcification (McConnaughey, 1995; McConnaughey and Whelan, 1997). Goreau (1959) suggested that H^+ secretion produced by calcification led to the production of CO_2 within the coelenteron, which was removed by photosynthesis according to the following equations:

$$Ca^{2+} + 2HCO_3^- \rightarrow CaCO_3 + CO_2 + H_2O \text{ (calcification)}, \quad (1)$$

$$CO_2 + H_2O \rightarrow CH_2O + O_2 \text{ (photosynthesis)}. \quad (2)$$

The hypothesis of McConnaughey and Whelan (1997) is similar to that of Goreau (1959) (coelenteric H^+ released by

$CaCO_3$ precipitation is used for coelenteric HCO_3^- dehydration to produce CO_2), but suggests that, in this way, calcification may stimulate photosynthesis by supplying CO_2. However, this last model was recently contradicted by studies performed by Gattuso et al. (2000), who demonstrated that it is possible to inhibit light-induced calcification without influencing photosynthesis. Allemand et al. (1998) have noted that all these hypotheses assume that the DIC source for photosynthesis is supplied from the coelenteron, which is probably not the case (Furla et al., 1998b; present study). They suggested an alternative hypothesis for light-enhanced calcification based on the titration of H^+ produced by calcification with the OH^- produced by photosynthesis (Furla et al., 1998b).

The present study confirms that, despite a decrease in coelenteric DIC concentration, there is a light-induced stimulation of calcification in *Stylophora pistillata*. Figs 4C and 7 reveal that the rate of calcification in the light is limited neither by external DIC concentration (K_m 220 μmol l^{-1}) nor by coelenteric DIC concentration (K_m 60 μmol l^{-1}), suggesting that there is no competition between photosynthesis and calcification for the external DIC source. These results contrast with the recent findings of Marubini and Thake (1999), who described stimulation of the calcification of the coral *Porites porites* by approximately 62 % after the addition of 2 mmol l^{-1} HCO_3^- in sea water.

Our results demonstrate that light-enhanced calcification is not dependent on a change in the supply of DIC, which remains mainly metabolic CO_2. Moreover, it is not an instantaneous phenomenon, but the stimulation of calcification requires activation of some unknown physiological mechanisms. This activation is responsible for the lag period observed. We hypothesise that changes in the pH/carbon state within the coelenteric cavity are part of this mechanism.

Concluding remarks

This paper clarifies such aspects of coral calcification as DIC sources, the mechanisms of DIC deposition into the skeleton, the interactions between photosynthesis and calcification and the activation of light-enhanced calcification. The conclusions, summarised in Fig. 8, are that the major source of DIC for coral calcification is metabolic CO_2 (independent of lighting conditions), and that DIC availability correlates with the presence of carbonic anhydrase activity probably localised within the calicoblastic cells, as previously suggested by Isa and Yamazato (1984). The secretion of DIC at the site of calcification is performed by an anion exchanger. After paracellular diffusion across the oral epithelial layers, 25–30 % of the DIC that originates from the external medium enters the calicoblastic cells by a DIDS-sensitive mechanism, which remains uncharacterised. There is no competition for DIC between photosynthesis and calcification of *Stylophora pistillata* microcolonies, calcification being saturated at low external and coelenteric DIC concentrations. Our results demonstrate the absence of an internal DIC pool for coral calcification. However, there is a 61-fold accumulation of DIC

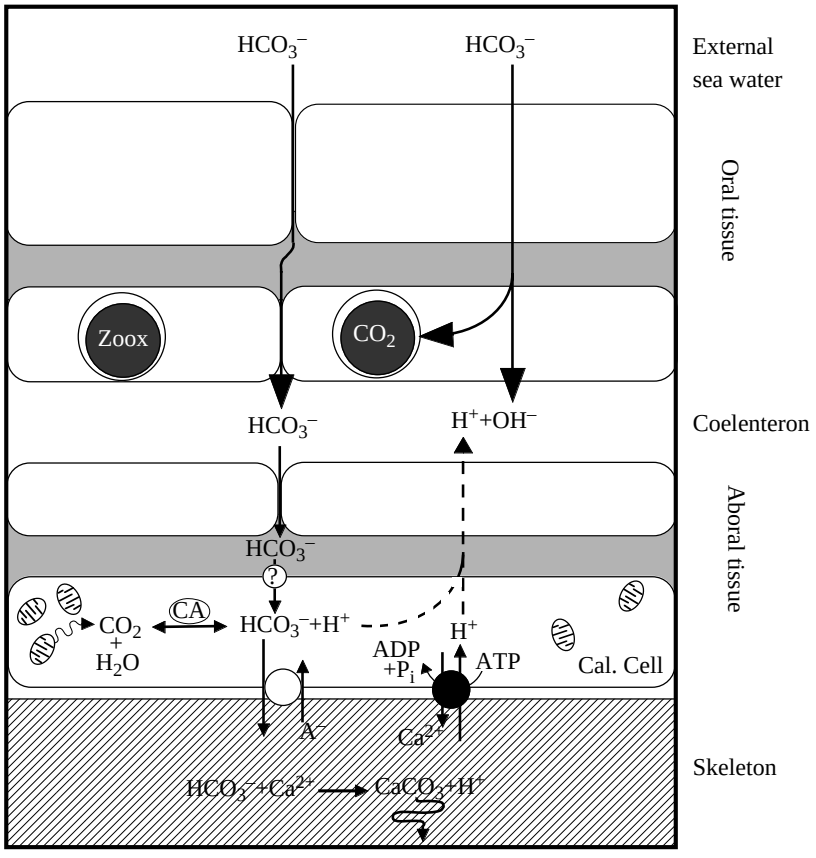

Fig. 8. Model of dissolved inorganic carbon (DIC) absorption for coral calcification and photosynthesis. Details are given in the text. Cal. Cell, calicoblastic cell; Zoox, zooxanthella; P_i, inorganic phosphate; CA, carbonic anhydrase.

within the tissue in the light compared with the DIC concentration of the external medium. This accumulation occurs through the CO_2-concentrating mechanism used for symbiont photosynthesis. Finally, we report a fourfold stimulation of calcification of *Stylophora pistillata* microcolonies in the presence of light, which appears after 10 min of illumination. We suggest that the coelenteric secretion of OH^- consecutive to external HCO_3^- absorption for symbiont photosynthesis favours stimulation of light-induced calcification.

We are grateful to G. Albini for performing the preliminary experiments. We also thank the Marine Station of Aqaba for facilitating the initial collection of corals, and the staff of the public aquarium of the Oceanographic Museum. We are also very grateful to Dr M. Frankignoulle for the free use of his 'CO_2' program and to Drs F. Marubini and R. J. Wilkins for helpful comments on the manuscript. This study was conducted as part of the Centre Scientifique de Monaco 1996–2000 research program. It was supported by the government of the Principality of Monaco and the Council of Europe (Open Partial Agreement on Major Natural and Technological Disasters).

References

Aizawa, K. and Miyachi, S. (1986). Carbonic anhydrase and CO_2-concentrating mechanisms in microalgae and cyanobacteria. *FEMS Microbiol.* **39**, 215–233.

Al-Moghrabi, S., Allemand, D. and Jaubert, J. (1993). Valine uptake by the scleractinian coral *Galaxea fascicularis*: characterization and effect of light and nutritional status. *J. Comp. Physiol.* B **163**, 355–362.

Al-Moghrabi, S., Goiran, C., Allemand, D., Speziale, N. and Jaubert, J. (1996). Inorganic carbon uptake for photosynthesis by the symbiotic coral/dinoflagellate association. II. Mechanisms for bicarbonate uptake. *J. Exp. Mar. Biol. Ecol.* **199**, 227–248.

Allemand, D., Furla, P. and Bénazet-Tambutté, S. (1998). Mechanisms of carbon acquisition for endosymbiont photosynthesis in Anthozoa. *Can. J. Bot.* **76**, 925–941.

Allemand, D. and Grillo, M.-C. (1992). Biocalcification mechanisms in gorgonians. ^{45}Ca uptake and deposition by the Mediterranean red coral *Corallium rubrum*. *J. Exp. Zool.* **292**, 237–246.

Barnes, D. J. and Chalker, B. E. (1990). Calcification and photosynthesis in reef-building corals and algae. In *Coral Reefs* (ed. Z. Dubinsky), pp. 109–131. Amsterdam: Elsevier.

Barnes, D. J. and Crossland, C. J. (1977). Coral calcification: sources of error in radioisotope techniques. *Mar. Biol.* **42**, 119–129.

Barnes, D. J. and Crossland, C. J. (1978). Diurnal productivity and apparent ^{14}C calcification in the staghorn coral *Acropora acuminata*. *Comp. Biochem. Physiol.* **59**A, 133–138.

Barnes, D. J. and Lough, J. M. (1996). Coral skeletons: storage and recovery of environmental information. *Global Change Biol.* **2**, 569–582.

Bénazet-Tambutté, S., Allemand, D. and Jaubert, J. (1996a). Permeability of the oral epithelial layers in Cnidarians. *Mar. Biol.* **126**, 43–53.

Bénazet-Tambutté, S., Allemand, D. and Jaubert, J. (1996b). Inorganic carbon supply to symbiont photosynthesis of the sea anemone, *Anemonia viridis*: role of the oral epithelial layers. *Symbiosis* **20**, 199–217.

Borle, A. B. (1990). Measurement of calcium movement across membranes: kinetic analysis and conceptualization. In *Intracellular Calcium Regulation* (ed. F. Bronner), pp. 19–75. New York: Wiley-Liss.

Bowes, G. and Salvucci, M. E. (1989). Plasticity in the photosynthetic carbon metabolism of submersed aquatic macrophytes. *Aquat. Bot.* **34**, 233–266.

Cabantchik, Z. I. and Greger, R. (1992). Chemical probes for anion transporters of mammalian cell membranes. *Am. J. Physiol.* **262**, C803–C827.

Chave, K. E., Smith, S. V. and Roy, K. J. (1975). Carbonate production by coral reefs. *Mar. Geol.* **12**, 123–140.

Crossland, C. J. (1980). Release of photosynthetically-derived organic carbon from a hermatypic coral, *Acropora* cf. *acuminata*. *Endocytobiol.* **1**, 163–171.

Drechsler, Z. and Beer, S. (1991). Utilization of inorganic carbon by *Ulva lactuca*. *Plant Physiol.* **97**, 1439–1444.

Druffel, E. R. M. (1997). Geochemistry of corals: Proxies of past ocean chemistry, ocean circulation and climate. *Proc. Natl. Acad. Sci. USA* **94**, 8354–8361.

Erez, J. (1978). Vital effect on stable-isotope composition seen in foraminifera and coral skeletons. *Nature* **273**, 199–202.

Forgac, M. (1989). Structure and function of vacuolar class of ATP-driven proton pumps. *Physiol. Rev.* **69**, 765–796.

Furla, P., Bénazet-Tambutté, S., Jaubert, J. and Allemand, D. (1998a). Diffusional permeability of dissolved inorganic carbon through the isolated oral epithelial layers of the sea anemone, *Anemonia viridis*. *J. Exp. Mar. Biol. Ecol.* **221**, 71–88.

Furla, P., Bénazet-Tambutté, S., Jaubert, J. and Allemand, D. (1998b). Functional polarity of the tentacle of the sea anemone *Anemonia viridis*: role in inorganic carbon acquisition. *Am. J. Physiol.* **274**, R303–R310.

Furla, P., Orsenigo, M. N. and Allemand, D. (2000). Involvement of H^+-ATPase and carbonic anhydrase in inorganic carbon absorption for endosymbiont photosynthesis. *Am. J. Physiol.* **278**, R870–R881.

Gates, R. D. and Edmunds, P. J. (1999). The physiological mechanisms of acclimatization in tropical reefs corals. *Am. Zool.* **39**, 30–43.

Gattuso, J.-P., Allemand, D. and Frankignoulle, M. (1999). Photosynthesis and calcification at cellular, organismal and community levels in coral reefs: A review on interactions and control by carbonate chemistry. *Am. Zool.* **39**, 160–183.

Gattuso, J.-P., Reynaud, S., Bourge, I., Furla, P., Romaine-Lioud, S., Frankignoulle, M. and Jaubert, J. (2000). Calcification does not stimulate photosynthesis in the zooxanthellate scleractinian coral *Stylophora pistillata*. *Limnol. Oceanogr.* **45**, 246–250.

Goiran, C., Al-Moghrabi, S., Allemand, D. and Jaubert, J. (1996). Inorganic carbon uptake for photosynthesis by the symbiotic coral/dinoflagellate association. I. Photosynthetic performances of symbionts and dependence on sea water bicarbonate. *J. Exp. Mar. Biol. Ecol.* **199**, 207–225.

Goreau, T. F. (1959). The physiology of skeleton formation in corals. I. A method for measuring the rate of calcium deposition by corals under different conditions. *Biol. Bull.* **116**, 59–75.

Goreau, T. F. (1961). On the relation of calcification to primary productivity in reef building organisms. In *The Biology of Hydra*

and of Some Other Coelenterates (ed. H. M. Lenhoff and W. F. Loomis), pp. 269–285. Coral Gables, Florida: University of Miami Press.

Goreau, T. J. (1977). Coral skeletal chemistry: physiological and environmental regulation of stable isotopes and trace metals in *Montastrea annularis*. *Proc. R. Soc. Lond. B* **196**, 291–315.

Ilundain, A. (1992). Intracellular pH regulation in intestinal and renal epithelial cells. *Comp. Biochem. Physiol.* **101**A, 413–424.

Ip, Y. K., Lim, A. L. L. and Lim, R. W. L. (1991). Some properties of calcium-activated adenosine triphosphatase from the hermatypic coral *Galaxea fascicularis. Mar. Biol.* **111**, 191–197.

Isa, Y. and Yamazato, K. (1984). The distribution of carbonic anhydrase in a staghorn coral *Acropora hebes* (Dana). *Galaxea* **3**, 25–36.

Johnston, I. S. (1980). The ultrastructure of skeletogenesis in zooxanthellate corals. *Int. Rev. Cytol*. **67**, 171–214.

Kühl, M., Cohen, Y., Dalsgaard, T., Jorgensen, B. B. and Revsbech, N. P. (1995). Microenvironment and photosynthesis of zooxanthellae in scleractinian corals studied with microsensors for O_2, pH and light. *Mar. Ecol. Prog. Ser*. **117**, 159–172.

Leggat, W., Badger, M. R. and Yellowlees, D. (1999). Evidence for an inorganic carbon-concentrating mechanism in the symbiotic dinoflagellate *Symbiodinium* sp. *Plant Physiol.* **121**, 1247–1255.

Lowry, O. H., Rosebrough, N. J., Farr, A. L. and Randall, R. J. (1951). Protein measurement with the folin phenol reagent. *J. Biol. Chem.* **193**, 265–275.

Lucas, J. M. and Knapp, L. W. (1997). A physiological evaluation of carbon sources for calcification in the octocoral *Leptogorgia virgulata* (Lamarck). *J. Exp. Biol*. **200**, 2653–2662.

Marshall, A. T. (1996). Calcification in hermatypic and ahermatypic corals. *Science* **271**, 637–639.

Marubini, F. and Thake, B. (1999). Bicarbonate addition promotes coral growth. *Limnol. Oceanogr.* **44**, 716–720.

McConnaughey, T. (1995). Ion transport and the generation of biomineral supersaturation. *Bull. Inst. Oceanogr*. **14**, 1–18.

McConnaughey, T. A. and Whelan, J. F. (1997). Calcification generates protons for nutrient and bicarbonate uptake. *Earth-Sci. Rev.* **42**, 95–117.

Mueller, E. (1984). Effects of a calcium channel blocker and an inhibitor of phosphodiesterase on calcification in *Acropora formosa. Adv. Reef Sci. Book of abstracts*, Miami, Florida. 87–88 (abstracts).

Palmqvist, K., Sjöberg, S. and Samuelsson, G. (1988). Induction of inorganic carbon accumulation in the unicellular green algae *Scenedesmus obliquus* and *Chlamydomonas reinhardtii*. *Plant Physiol.* **87**, 437–442.

Pearse, V. B. (1970). Incorporation of metabolic CO_2 into coral skeleton. *Nature* **228**, 383.

Shick, J. M. (1990). Diffusion limitation and hyperoxic enhancement of oxygen consumption in zooxanthellate sea anemones, zoanthids and corals. *Biol. Bull.* **179**, 148–158.

Smith, L. (1978). Coral reef area and the contributions of reefs to processes and resources of the world's oceans. *Nature* **273**, 225–226.

Smith, R. G. (1988). Inorganic carbon transport in biological systems. *Comp. Biochem. Physiol.* **90**B, 639–654.

Tambutté, É., Allemand, D., Mueller, E. and Jaubert, J. (1996). A compartmental approach to the mechanism of calcification in hermatypic corals. *J. Exp. Biol.* **199**, 1029–1041.

Yellowlees, D., Dionisio-Sese, M. L., Masuda, K., Maruyama, T., Abe, T., Baillie, B., Tsuzuki, M. and Miyachi, S. (1993). Role of carbonic anhydrase in the supply of inorganic carbon to the giant clam–zooxanthellate symbiosis. *Mar. Biol*. **115**, 605–611.

Zoccola, D., Tambutté, É., Sénégas-Balas, F., Michiels, J.-F., Failla, J.-P., Jaubert, J. and Allemand., D. (1999). Cloning of a calcium channel α1 subunit from the reef-building coral, *Stylophora pistillata*. *Gene* **227**, 157–167.